

# Variations and relations between chlorophyll concentrations and physical-ecological processes near the West Antarctic Peninsula

WU Shuang<sup>1</sup>, ZHANG Zhaoru<sup>1,2,3,4\*</sup> & WANG Chuning<sup>1</sup>

<sup>1</sup> School of Oceanography, Shanghai Jiao Tong University, Shanghai 200030, China;

<sup>2</sup> Key Laboratory of Polar Science, MNR, Polar Research Institute of China, Shanghai 200136, China;

<sup>3</sup> Key Laboratory of Polar Ecosystem and Climate Change, Ministry of Education, Shanghai Jiao Tong University, Shanghai 200030, China;

<sup>4</sup> Shanghai Key Laboratory of Polar Life and Environment Sciences, Shanghai Jiao Tong University, Shanghai 200030, China

Received 1 July 2023; accepted 2 October 2023; published online 30 December 2023

**Abstract** The West Antarctic Peninsula (WAP) region is one of the most productive marine ecosystems in the Southern Ocean that support the food web for phytoplankton, krill spawning or recruitment and several krill consumers at higher-trophic level like penguins and Antarctic fur seals. Characterized by channels and islands, the complex topography of the WAP generates interconnected circulation patterns, strongly influencing vertical stratification, nutrient availability and distribution of marine organisms. Additionally, rapid climate change associated with major climate modes like the Southern Annular Mode (SAM) and El Niño-Southern Oscillation (ENSO) has significant effects on long-term variations of physical environments and biological production. The objective of this study is to reveal the spatial-temporal variations of phytoplankton biomass in the WAP region and the modulating physical-ecological processes. By using 9-year hydrographic and ecological data of five transects collected by the Palmer Long-Term Ecosystem Research, the horizontal and vertical distributions of several physical and ecological properties, with a particular focus on chlorophyll (Chl) concentration were explored. Regression analysis among area-averaged properties and properties at single stations was performed to reveal the relationship between the interannual variations of physical and ecological processes. The correlation results showed that Chl concentration exhibited a positive relationship with both the circumpolar deep water (CDW) intrusion and vertical stratification, but showed a negative correlation with SAM at some specific stations. However, certain processes or mechanisms may only be dominant for specific stations and not applicable to the entire region. No single physical or ecological factors have been found to significantly influence the Chl distribution throughout the WAP region, which may be attributed to the heterogeneity of sea ice conditions, geometry and hydrodynamic features as well as variations in nutrient sources.

**Keywords** West Antarctic Peninsula, phytoplankton productivity, temporal-spatial variations, physical-ecological coupling processes

**Citation:** Wu S, Zhang Z R, Wang C N. Variations and relations between chlorophyll concentrations and physical-ecological processes near the West Antarctic Peninsula. *Adv Polar Sci*, 34(4): 262-271, doi: 10.12429/j.advps.2023.0010

## 1 Introduction

The West Antarctic Peninsula (WAP) is a biological hotspot for phytoplankton primary productivity and krill

spawning or recruitment, which support high trophic-level predators. The complex bathymetry of the WAP, including numerous islands and channels, generates a series of circulation systems and mesoscale eddies that enhance vertical mixing, nutrient supply or energy exchange (Schofield et al., 2018). The WAP is significantly affected by the Antarctic Circumpolar Current (ACC), which plays a key

\* Corresponding author, ORCID: 0000-0001-6125-8660, E-mail: zrzhang@sjtu.edu.cn

role in the transport of heat, nutrients as well as in the distributions of marine organisms (Loeb et al., 2010). The WAP region has also experienced rapid climate change associated with the variations of major climate modes, such as the Southern Annular Mode (SAM) and the El Niño-Southern Oscillation (ENSO) (Li et al., 2015). SAM is characterized by opposite anomalies of sea-level pressure in the high and mid latitudes of the southern hemisphere (Marshall, 2003), which is the dominant mode of extratropical climate variability in the southern hemisphere. Understanding changes in the WAP ecosystem requires knowledge of mechanisms linking the physical and ecological processes.

Several studies have examined the long-term variations of biological production and their connection with physical environments in specific regions in the WAP region. For example, Schofield et al. (2018) investigated the long-term changes in the mixed layer depth (MLD), sea ice, mixed layer depth and phytoplankton productivity separately in the northern and southern regions sampled by the Palmer Long-Term Ecological Research (PAL-LTER) program (Figure 1). Zhang et al. (2020) revealed the mechanisms for SAM to affect the interannual variability of physical processes near the Elephant Islands and South Shetland Islands of the WAP, such as MLD, the intrusion of nutrient-rich circumpolar deep water (CDW), irradiance and phytoplankton biomass. Saba et al. (2014) assessed how climate modes affect the interannual variations of phytoplankton and Antarctic krill biomasses at PAL-LTER stations in coastal regions, and found negative correlation between the interannual variations of summer chlorophyll (Chl) concentration and SAM due to changes in ice thickness, wind strength, salinity gradients and water stability. However, their studies only analyzed data from two stations, and the applicability of the conclusions and mechanisms to larger areas is uncertain. In this work, we use long-term data collected by the PAL-LTER program covering coastal regions, continental shelf and continental slope of the WAP, and aim to explore factors and mechanisms that could explain the distribution of Chl concentration over wider areas.

The objective of this study is to investigate and quantify the impacts of coupled physical-ecological processes on the spatial-temporal patterns of Chl concentration in the WAP region covered by the PAL-LTER program. Five transects crossing the shelf and slope areas were selected, and the horizontal and vertical distributions of several physical-ecological properties, with a particular focus on Chl concentration, were studied over nine years. Factors controlling the variation of the phytoplankton biomass were investigated.

## 2 Data and methods

### 2.1 Data

The LTER program was founded in 1980 by the

National Science Foundation, United States with the recognition that long-term research could help understand the mechanisms of ecological science. Palmer Station was designated as polar biome LTER sites in 1990 to focus on the pelagic marine ecosystem along the WAP. A major component of PAL-LTER program is an annual ship survey conducted each austral summer. The survey included a series of cross-shelf transects that covered a north-south gradient (Figure 1). The research area is centered on a 180000 km<sup>2</sup> region, with an elevation range from 10 m on land to 2000 m below sea level. This forms an oceanic sampling grid along the shore, roughly parallel to the Peninsula.

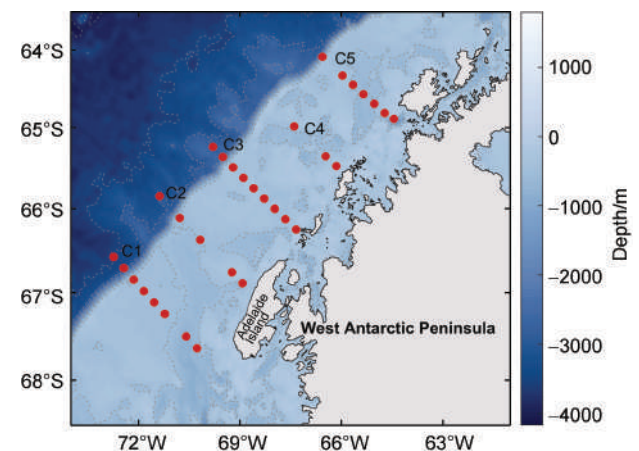


**Figure 1** Map of study sites along the West Antarctic Peninsula region in the PAL-LTER survey area. Red circles mark the locations of sampled stations on the five transects C1–C5.

This study used long-term hydrographic and ecological data collected by PAL-LTER, and all data are publicly available at the website (<http://pal.lternet.edu/data>). The hydrographic data consisted of salinity, temperature and density. The ecological data consisted of Chl concentration and nutrient concentrations at different depths. The surface Chl concentration at each station was represented by the Chl concentration closest to the depth of 13 m. The surface nutrient concentrations were determined using the same criteria.

By considering the integrity of hydrographic data and ecological data, we used data from 9 years, including 1995, 1999–2000, 2001–2002, 2004 and 2006–2008 to explore the temporal-spatial distributions of Chl concentration and the controlling physical-biogeochemical factors. The 32 red circles in Figure 1 represent the stations with sampling data over all of the 9 years. Due to the impossibility of precise repeated sampling at absolutely identical location, stations with distances less than 0.1 degrees in latitude and longitude (approximately 4.5 km apart) are considered to be the same station.

The annual SAM indices (SAMI) used in this study were calculated based on the zonal pressure difference between the latitudes of 40°S and 65°S (Marshall, 2003),

and the data were obtained from the British Antarctic Survey, a component of the National Environment Research Council (<http://www.nerc-bas.ac.uk/icd/gjma/sam.html>). SAMI was analyzed for correlations with physical processes, such as vertical stratification and CDW intrusion, as well as with biological properties, including the concentration of surface Chl, nitrate, phosphate and silicate.

## 2.2 Methods

The strength of stratification can be characterized by the buoyancy frequency ( $N^2$ )

$$N^2 = -\frac{g}{\rho} \frac{\partial \rho}{\partial z}, \quad (1)$$

where  $\rho$  is the density of water,  $z$  is the vertical coordinate (m),  $\frac{\partial \rho}{\partial z}$  represents the vertical gradient of the water density,  $g$  is the gravitational acceleration. Larger  $N^2$  means stronger stratification or weaker mixing of the water column. The maximum buoyancy frequency throughout the water column at a station is denoted by  $N_{\max}^2$ . MLD is defined as the depth at which the potential density of seawater differs by  $0.03 \text{ kg}\cdot\text{m}^{-3}$  from the surface potential density (Dong et al., 2008). The depth where the potential density equals  $27.6 \text{ kg}\cdot\text{m}^{-3}$  is defined as the core depth of CDW, and potential temperature at this depth  $T_{\text{CDW}}$  was extracted (Loeb et al., 2010). Higher  $T_{\text{CDW}}$  indicates stronger CDW intrusion.

In this study, linear regression was used to analyze the correlation between the interannual variability of two variables, with regression coefficients  $\beta_0$  and  $\beta_1$  indicating the intercept and slope of fitted linear curve and  $R$  indicating the correlation coefficient (Thomson and Emery, 2014). The correlation is considered significant when the  $p$ -value is no greater than 0.05. Additionally, the Pearson-residuals statistical method is utilized to test whether the residuals conform to the statistics assumption of a normal distribution and to remove outlier data that significantly deviates from the regression model (Wasserman, 2004).

## 3 Results

### 3.1 Temporal-spatial patterns of Chl concentration and the relation with buoyancy frequency

The spatial patterns of surface Chl concentration for each of the 9 years are displayed in Figure 2. Surface Chl concentrations were higher in nearshore areas, generally above  $0.8 \text{ mg}\cdot\text{m}^{-3}$ , and decreased offshore, generally below  $0.5 \text{ mg}\cdot\text{m}^{-3}$  at the northern end of the transects. Especially near the Adelaide Island, Chl concentrations can reach up to 10 and no less than  $2 \text{ mg}\cdot\text{m}^{-3}$ . Additionally, there was no clear spatial trend detected for the surface Chl concentration on either transect.

In terms of temporal variations, the surface Chl

concentrations were generally highest in 2006, with concentrations up to  $10 \text{ mg}\cdot\text{m}^{-3}$  and mostly around  $5 \text{ mg}\cdot\text{m}^{-3}$ . The Chl concentrations were also relatively high in 1995 and 2007, ranging from  $0.5$  to  $5 \text{ mg}\cdot\text{m}^{-3}$  and  $0.2$  to  $8 \text{ mg}\cdot\text{m}^{-3}$ , respectively. Conversely, the concentrations were lowest in 1999, with values down to  $0.1 \text{ mg}\cdot\text{m}^{-3}$  and mostly around  $0.5 \text{ mg}\cdot\text{m}^{-3}$ , ranging from  $0.1$  to  $3 \text{ mg}\cdot\text{m}^{-3}$ . In the rest of the years, surface Chl concentrations were intermediate, ranging from  $0.3$  to  $5 \text{ mg}\cdot\text{m}^{-3}$ . The temporal patterns of the maximum buoyancy frequency (hereafter denoted by  $N_{\max}^2$ ) for the 9 years are shown in Figure 3.  $N_{\max}^2$  generally reached its highest level in 2006, with frequencies up to  $10^{-2.6} \text{ s}^{-2}$  and minimum values greater than  $10^{-3.4} \text{ s}^{-2}$ . The higher frequencies indicate stronger stratification. The lowest  $N_{\max}^2$  was observed in 1995, with frequencies down to  $10^{-4} \text{ s}^{-2}$ , mostly around  $10^{-3.8} \text{ s}^{-2}$ , which was significantly smaller than frequencies in the other 8 years, indicating the strongest vertical mixing and weakest stability. The second lowest  $N_{\max}^2$  was observed in 2008, with concentrations ranging from  $10^{-3.8}$  to  $10^{-3.1} \text{ s}^{-2}$ . In the rest of the years,  $N_{\max}^2$  and water column stability were intermediate. There was no obvious spatial trend detected for  $N_{\max}^2$  from nearshore to offshore.

As mentioned in Section 2, among all of the PAL-LTER stations, 32 stations have data over all 9 years. For each year, the surface Chl concentration and  $N_{\max}^2$  were averaged over the 32 stations, and then the correlation between interannual variations of region-average Chl and  $N_{\max}^2$  was analyzed. The two quantities had a positive but insignificant correlation ( $P = 0.17$ ). We then examined the correlation at each of the 32 stations, using the full-length of data at each station, and the results indicated a significant positive relationship between the two variables at 6 stations (Figure 4), suggesting that in these areas the ocean stratification is an important modulating factor for the interannual variability of summer phytoplankton biomass, which could relate to light conditions, phytoplankton accumulation and iron limitation.

### 3.2 The relation between Chl concentration and extent of CDW

Another potential physical factor affecting the phytoplankton biomass is the intrusion and extent of the nutrient-rich CDW, which is indicated by the distribution of  $T_{\text{CDW}}$  (Figure 5). In terms of temporal variation,  $T_{\text{CDW}}$  attained its peak values in 2007, with a range from  $0.3$  to  $1.6 \text{ }^\circ\text{C}$  (except for one station that was below  $0 \text{ }^\circ\text{C}$ ), indicating stronger intrusion and wider coverage of CDW in the study area. The second highest  $T_{\text{CDW}}$  occurred in 2006, ranging from  $0.1$  to  $1.4 \text{ }^\circ\text{C}$ , which was lower than that observed in 2007 near offshore regions.  $T_{\text{CDW}}$  was generally at its lowest value in 2004 with temperature below  $-0.3 \text{ }^\circ\text{C}$  and in most areas around  $-0.1 \text{ }^\circ\text{C}$  (with an exception on transect C5). The second lowest  $T_{\text{CDW}}$  was observed in 1999, with temperatures ranging from  $0$  to  $0.6 \text{ }^\circ\text{C}$ , mostly

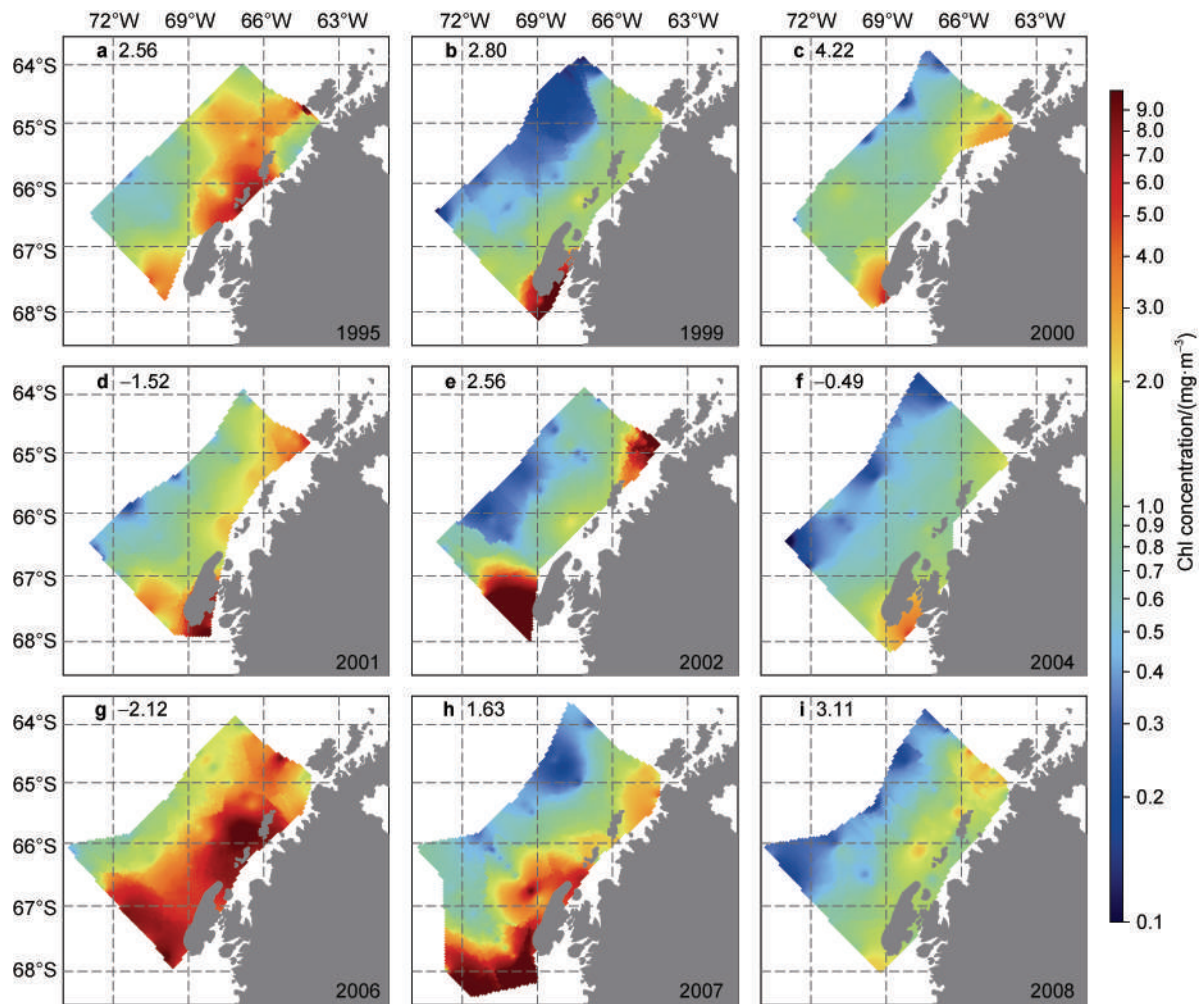


**Figure 2** Distributions of surface Chl concentration in the PAL-LTER survey area over the nine selected years. The summer SAMI values are labeled in the upper left corner of the panels, and the years are labeled in the lower right corner.

around  $0.1\text{ }^{\circ}\text{C}$ . Spatially,  $T_{\text{CDW}}$  exhibited higher values in the offshore areas, generally above  $0.8\text{ }^{\circ}\text{C}$  at the northern ends of the transects and below  $0.5\text{ }^{\circ}\text{C}$  nearshore.

The interannual variations of surface Chl concentration and  $T_{\text{CDW}}$  averaged over stations with data covering all of the 9 years are significantly correlated ( $R = 0.81$ ,  $P = 0.01$ ). We then examined such correlation for each station, and found positive relationship at 3 stations and negative relationship at 2 stations (Figure 6). The occurrence of CDW in the WAP shelf area was associated with increased primary production (Prézelin et al., 2004), which can be attributed to the supplementation of macronutrients and dissolved iron (dFe) to the upper ocean that driven by CDW intrusion.

### 3.3 Chl concentration and nutrients

#### 3.3.1 Spatial-temporal patterns of nitrate concentration

The spatial distribution of surface nitrate concentration in each of the 9 years is shown in Figure 7. The surface nitrate concentrations were overall highest in 1995 and

2000, ranging from  $18$  to  $25\text{ }\mu\text{mol}\cdot\text{L}^{-1}$ . The surface nitrate concentrations were lowest in 2007, with concentrations ranging between  $6$  and  $18\text{ }\mu\text{mol}\cdot\text{L}^{-1}$ , areas adjacent to the Adelaide Island were characterized by surface nitrate concentration below  $8\text{ }\mu\text{mol}\cdot\text{L}^{-1}$ . In the other years, surface nitrate concentrations had intermediate values ranging from  $15$  to  $23\text{ }\mu\text{mol}\cdot\text{L}^{-1}$ . For spatial distributions, surface nitrate concentrations increased offshore (except for 1995 and 2006). Transect C1 exhibited the lowest surface nitrate concentrations among all transects in more than half of the years (1999, 2000, 2002, 2004, 2006 and 2007).

#### 3.3.2 Spatial-temporal patterns of phosphate concentration

The spatial patterns of surface phosphate concentration in the 9 years are shown in Figure 8. The phosphate concentrations were found to be highest in 2008 and 2000, ranging from  $1.5$  to  $1.8\text{ }\mu\text{mol}\cdot\text{L}^{-1}$ . The lowest phosphate concentrations were observed in 1995 and 2007, ranging from  $0.6$  to  $1.6\text{ }\mu\text{mol}\cdot\text{L}^{-1}$  (excluding three stations in 1995 exceeding  $1.8\text{ }\mu\text{mol}\cdot\text{L}^{-1}$ ). Other low surface phosphate concentrations were observed in 2001 and 2004, with

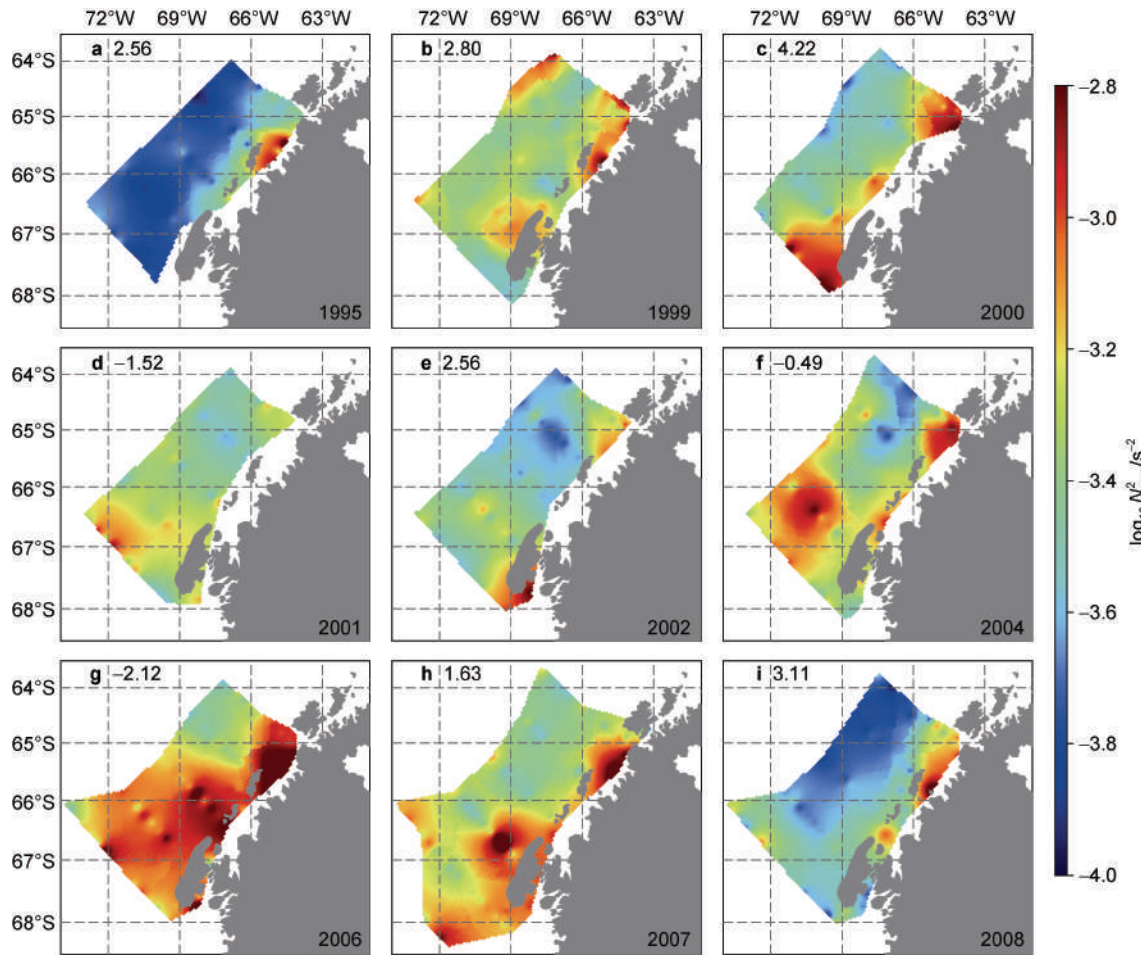


**Figure 3** Distributions of maximum buoyancy frequency in the PAL-LTER study area. The summer SAMI value in each year is shown in the upper left corner.

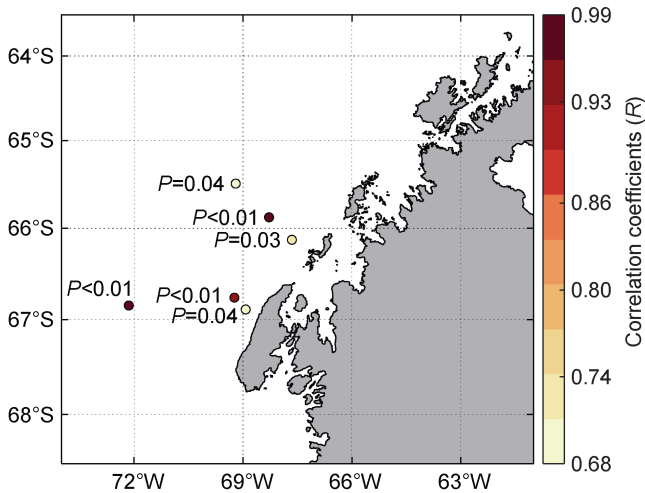


**Figure 4** Relationship between the interannual variations of summer time Chl concentration and  $N_{max}^2$  at different stations. Dots mark the stations where there exist significant correlations between the two variables; color represents the value of correlation coefficients ( $R$ ) at each station, and the  $p$ -value ( $P$ ) of the correlation is labeled in the figure.

values mostly around  $1.2 \mu\text{mol}\cdot\text{L}^{-1}$ . In the other years, surface phosphate concentrations were intermediate, ranging from  $0.8$  to  $1.6 \mu\text{mol}\cdot\text{L}^{-1}$ .

It is noted that surface Chl concentrations were greatest in 2006, followed by 2001 and 1995, and lowest in 2008 and 2000 (Figure 2), which is generally contrary to the temporal variation of phosphate concentrations as analyzed above. This was particularly evident on Transect C1 during 2002, 2007 and 1995. The western transect C1 were characterized by a sharp increase in the concentration of phosphate, which rose from below  $0.8$  to over  $1.1 \mu\text{mol}\cdot\text{L}^{-1}$ , and a sharp decrease in Chl concentration, which declined from more than  $2$  to less than  $0.8 \text{ mg}\cdot\text{m}^{-3}$ . In 2002, the sites with sharp changes in phosphate and Chl concentrations were observed at  $67.38^\circ\text{S}$ ,  $70.91^\circ\text{W}$  along transect C1. As the longitude and latitude difference between these two stations was less than  $0.1^\circ$ , they can be considered as the same station. Similarly, the sites were observed at  $67.64^\circ\text{S}$ ,  $70.27^\circ\text{W}$  in 1995, and then observed at  $67.90^\circ\text{S}$ ,  $69.62^\circ\text{W}$  in 2007 along the same transect. Further quantitative analysis of the relationship between the interannual variations of surface Chl concentration and surface nutrient concentration will be presented in the following sections.

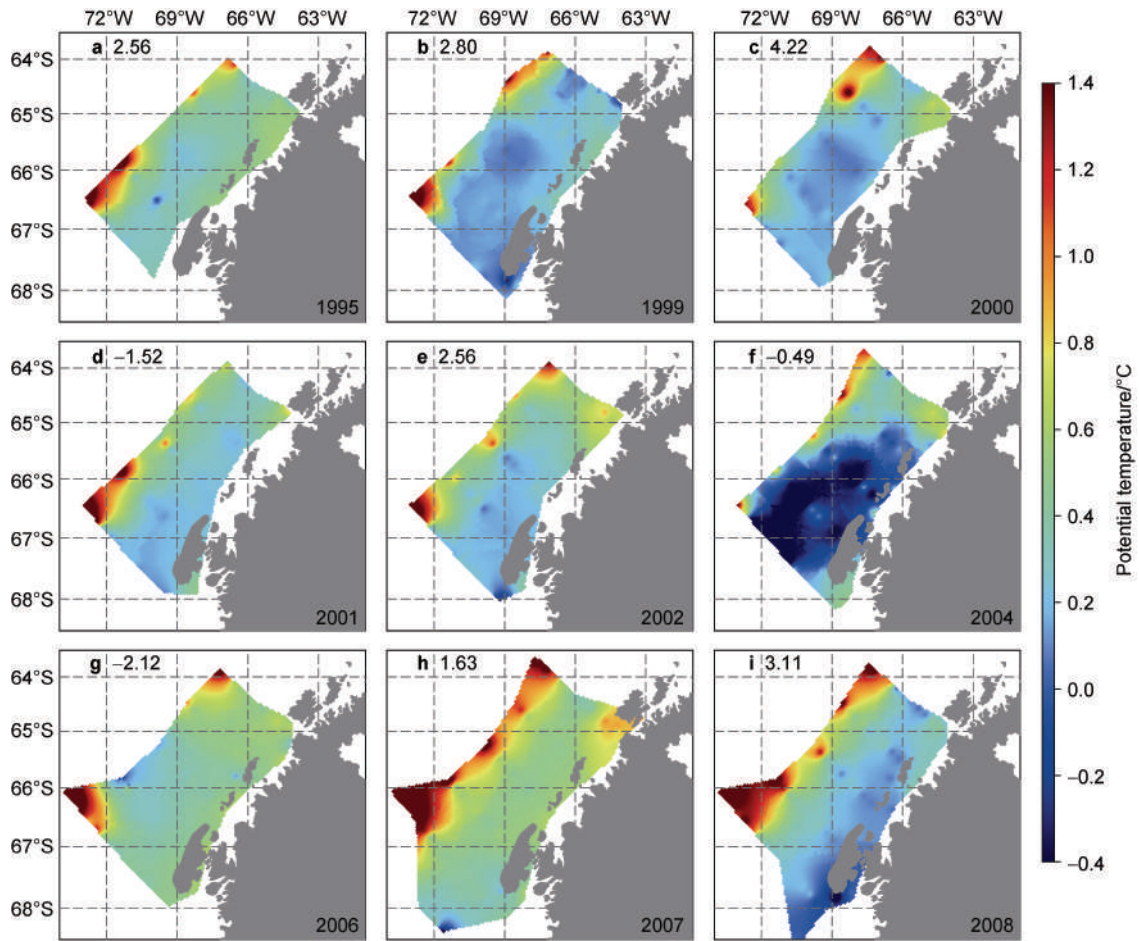


**Figure 5** Distributions of temperature on the potential density surface of  $27.6 \text{ kg}\cdot\text{m}^{-3}$  ( $T_{CDW}$ ) in the PAL-LTER survey area for the 9 years. The annual SAMI value in each year is shown in the upper left corner.

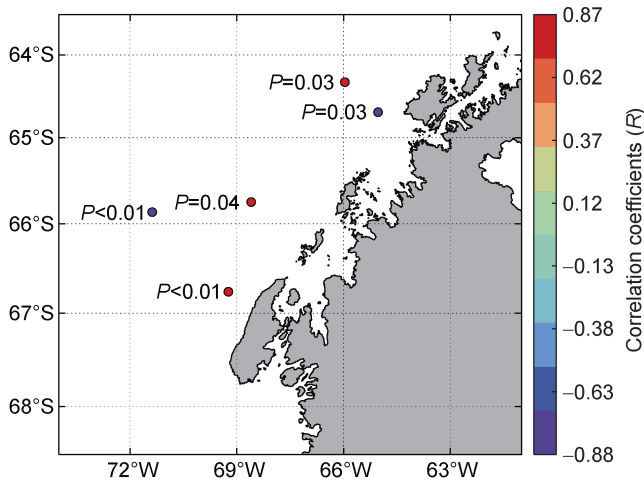


**Figure 6** Relationship between interannual variations of summer time Chl concentration and  $T_{CDW}$  at different stations. Dots mark the stations where there exist significant correlations between the two variables. Color represents the value of correlation coefficients ( $R$ ) at each station, and the  $p$ -value ( $P$ ) of the correlation is labeled in the figure.

### 3.3.3 Spatial-temporal patterns of silicate concentration

Figure 9 illustrates the spatial patterns of surface silicate concentration for each of the 9 years. The highest surface silicate concentrations were observed in 1995 and 2007, with values mostly ranging between  $60$  to  $85 \mu\text{mol}\cdot\text{L}^{-1}$ . The surface silicate concentrations were lowest in 1999, with concentrations ranging from  $30$  to  $65 \mu\text{mol}\cdot\text{L}^{-1}$  and mostly around  $45 \mu\text{mol}\cdot\text{L}^{-1}$ . In other years, surface silicate concentrations ranged from  $40$  to  $70 \mu\text{mol}\cdot\text{L}^{-1}$ . In terms of spatial distributions, the surface silicate concentrations were generally higher in the nearshore area, with concentrations above  $60 \mu\text{mol}\cdot\text{L}^{-1}$  (except for 1999), and decreased offshore with concentrations generally below  $50 \mu\text{mol}\cdot\text{L}^{-1}$  at the northern ends of the transects (except for 1995 and 2006). Additionally, Transect C5 exhibited the highest surface silicate concentrations among all transects in more than half of the years (1995, 1999, 2000, 2006, and 2007).

### 3.3.4 Correlations between the Chl concentration and nutrient concentrations

Correlations between interannual variations of surface Chl concentration and surface nutrient concentrations were

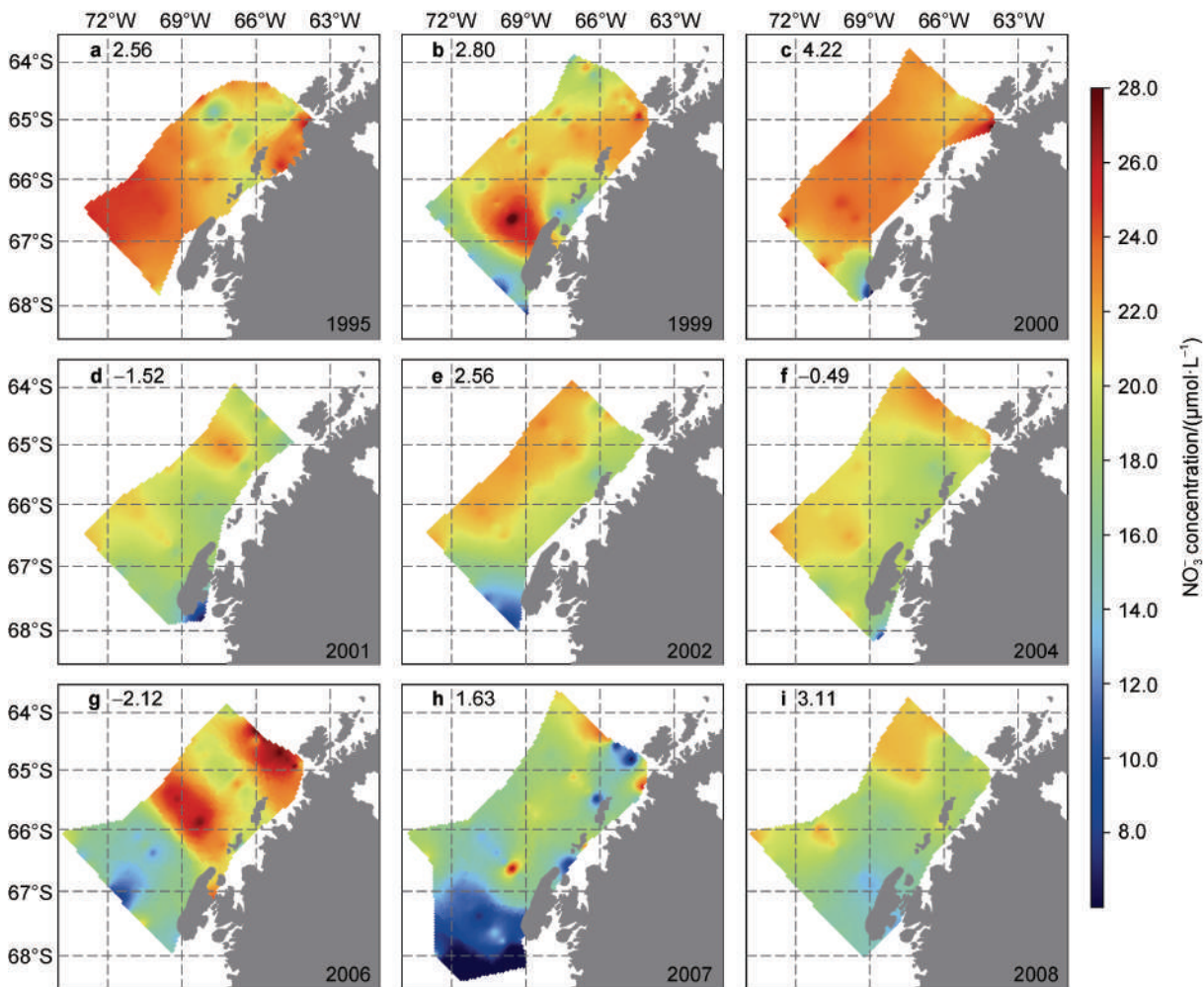


**Figure 7** Distributions of surface nitrate concentrations in the PAL-LTER survey area. The summer SAMI value in each year is shown in the upper left corner.

examined for the area mean and each station (Figure 10). For the area mean, there is no significant correlation between the Chl concentration and either nutrient concentration. For individual stations, there was one station with significant negative correlation between the Chl concentration and nitrate concentration, and three stations with significant positive correlations (Figure 10a). Significant negative correlation with phosphate concentrations was found at one station (Figure 10b), corresponding precisely to the site with sharp changes of phosphate and Chl concentrations identified in 2002. For the silicate, there were two sites showing significant positive or negative correlations between Chl concentration and silicate concentration.

Among the stations that have significant relationship between Chl and nutrient concentrations as mentioned above, there is one station where Chl is both significantly correlated with nitrate and phosphate (on transect C1), and one station where Chl is both significantly correlated with nitrate and silicate. The discrepancies in the correlations between Chl concentration and different

nutrients will be addressed in the subsequent section.

## 4 Discussions and conclusions

To investigate the possible influence of the large-scale climate mode SAM on the interannual variation of surface Chl distribution, the correlation between Chl concentration and the summer SAM index was analyzed (Figure 11). The results showed a weak negative correlation between the two quantities for the regional average, with a  $p$ -value of 0.13. However, station-by-station analysis revealed a significant negative correlation between the two variables at two stations. The northern station (64.33°S, 65.96°W) coincided with one of the stations where Chl was positively correlated with  $T_{CDW}$  (Figure 6), which implied that Chl exhibited a positive relationship with CDW intrusion but showed a negative correlation with SAM at this specific station. The two stations that exhibited significant correlations between SAM and Chl do not overlap with the six stations that showed

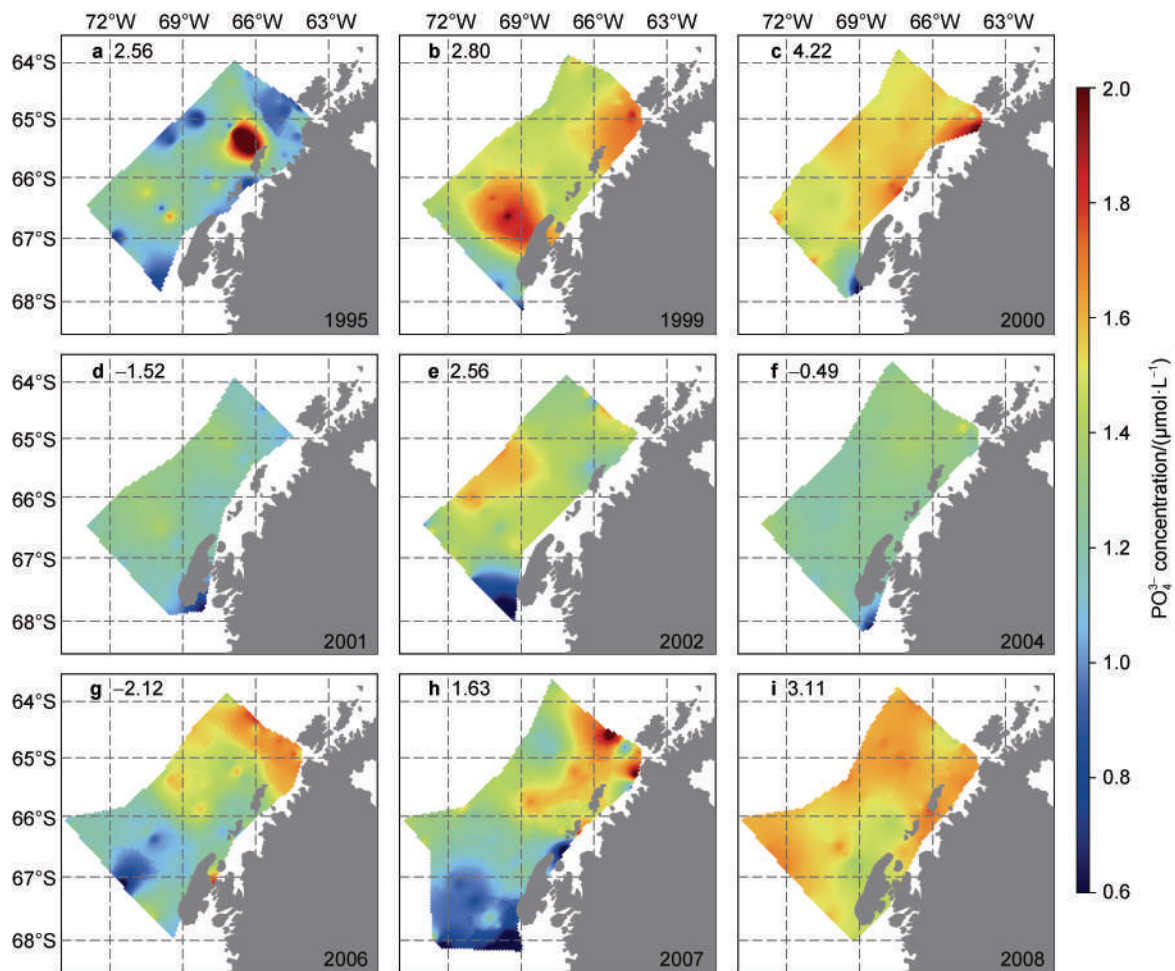


**Figure 8** Distributions of surface phosphate concentrations in the PAL-LTER study area for the 9 years. The summer SAMI in each year is shown in the upper left corner.

significant correlations between the buoyancy frequency and Chl concentration, which indicated that SAM did not directly regulate Chl distribution by influencing water column stability.

We also found that at one station (66.76°S, 69.24°W), Chl concentration had a significant positive correlation with both the  $N_{\max}^2$  and  $T_{\text{CDW}}$ , which means Chl concentration can be stimulated by enhanced vertical stratification and CDW intrusion at the specific station. The mechanisms between water column stratification and phytoplankton biomass could be related to light conditions and iron limitation. Enhanced vertical mixing can transport more phytoplankton into deeper layers below the euphotic zone, reducing the time available for photosynthesis in the surface layer and thereby decreasing productivity and biomass. On the contrary, increased stratification can enhance phytoplankton growth by increasing the light intensity in the surface layer. The positive promotion between  $T_{\text{CDW}}$  and Chl concentration can be attributed to the enhanced availability of nutrients in the surface water that derived from CDW intrusion. As CDW mainly flows along deep troughs on the Antarctic continental shelves, it can collect

dFe originating from sediments and then transport it to the upper water (Gerringa et al., 2012; Arrigo et al., 2017). More existence of CDW could also bring water with higher concentration of macronutrients like nitrate and phosphate to the upper ocean, helping promote phytoplankton growth (Venables et al., 2013; Saba et al., 2014).

Previous studies had revealed that SAM variability can affect Chl concentration in the WAP region both directly through wind-driven mixing (Saba et al., 2014) and indirectly through influencing CDW intrusion (Zhang et al., 2020). SAM variability influences the strength and position of the westerly winds. When SAM is in positive phase with higher index, the westerly winds strengthen and shift southward, pumping CDW up to shallower depths through upwelling. This leads to more intensive intrusion of CDW onto the continental shelves around Antarctica, bringing more nutrients and dissolved iron into the surface water and stimulating phytoplankton growth (Loeb et al., 2009). Our study indicates that the relations among SAM, CDW intrusion and Chl vary across the WAP region, which are strong in some areas but weak in other areas such as the PAL-LTER survey region. When analyzing the correlation



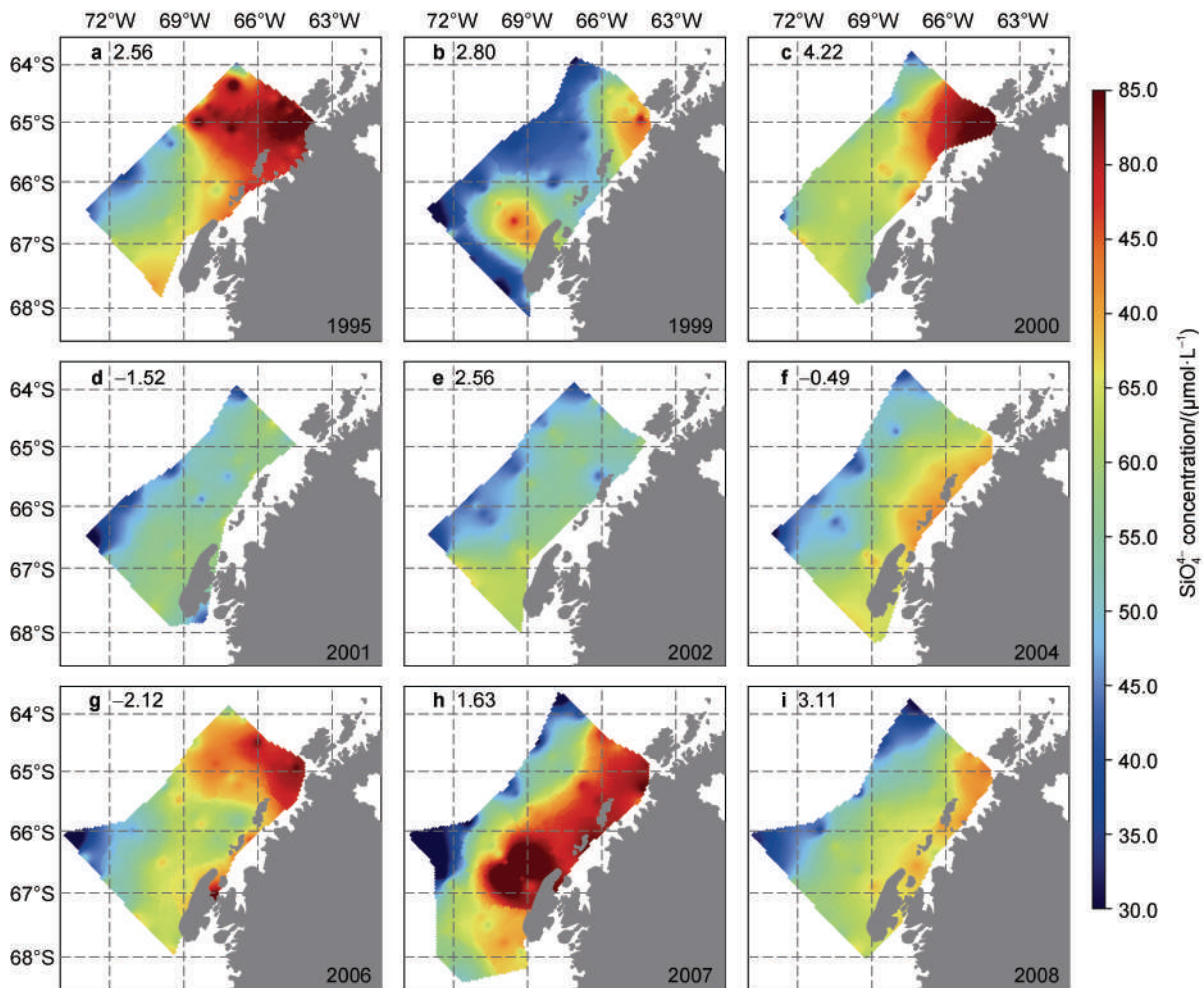


**Figure 9** Distributions of surface silicate concentrations in the PAL-LTER study area. The summer SAMI value in each year is shown in the upper left corner.

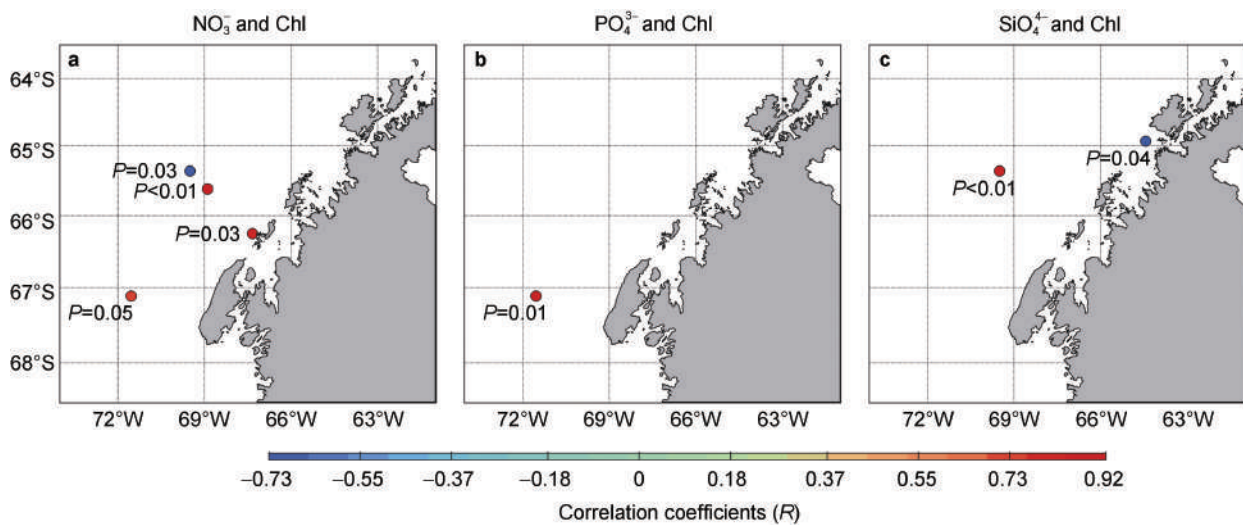


**Figure 10** Relationship between the interannual variations of summer time Chl concentration and concentrations of 3 individual nutrients at different stations. Dots mark the stations where there exist significant correlations between the Chl and nutrient concentrations, color represents the value of correlation coefficients ( $R$ ) at each station, and the  $p$ -value ( $P$ ) of the correlation is labeled in the figure.

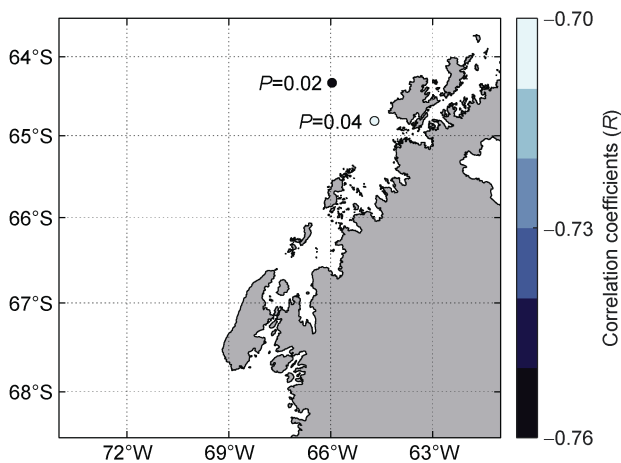


**Figure 11** Relationship between the interannual variations of summer time Chl concentration and summer SAMI at different stations. Dots mark the stations where there exist significant correlations between the two variables, color represents the value of correlation coefficients ( $R$ ) at each station, and the  $p$ -value ( $P$ ) of the correlation is labeled in the figure.

between  $T_{CDW}$  and surface Chl concentration, a significant positive correlation was found for the regional average of the two variables. However, inconsistencies emerged under station-by-station calculation, including three stations exhibiting positive correlations and two stations exhibiting negative correlations. This indicates that the impacts of physical-ecological processes may have significant spatial variations possibly due to nutrient sources.

Based on our analysis, no single physical or ecological factor has been found to significantly influence the regional Chl distribution throughout the WAP. We did not find that SAM exerted unified control over the spatial-temporal patterns of physical and ecological processes like vertical mixing, CDW intrusion, and nutrient concentration in our study region. Even though there were significant correlations at particular stations between partial variables, such as the notable relationship between Chl and stratification frequency and relationship between CDW intrusion and SAM at specific locations, these relations do not apply to a wider region. This may be attributed to the fact that physical-ecological processes vary across the study area. For example, the role of stratification on the nutrient distributions in the surface layer depends on the sources and transportation pathways of nutrients. Changes in SAM can induce changes in multiple physical processes, such as vertical mixing, CDW intrusion, sea ice freezing/melting. The role of one process on Chl concentration may be cancelled by effects from other processes, and result in weak correlation of Chl concentration with either process. This study indicates that the controlling mechanisms for Chl concentration in the WAP region need to be explored locally, and it should be cautious to extend the relationship derived at one place to wider regions.

**Acknowledgments** This work is supported by the National Natural Science Foundation of China (Grant nos. 41941008 and 41876221) and the National Key Research and Development Program of China (Grant no. 2022YFC2807601). We appreciate two anonymous reviewers and Associate Editor Dr. Jianfang Chen for their constructive comments that have further improved the manuscript.

## References

- Arrigo K R, Van Dijken G L, Alderkamp A C, et al. 2017. Early spring phytoplankton dynamics in the western Antarctic Peninsula. *J Geophys Res Oceans*, 122(12): 9350-9369, doi: 10.1002/2017JC013281.
- Dong S, Sprintall J, Gille S T, et al. 2008. Southern Ocean mixed-layer depth from Argo float profiles. *J Geophys Res Oceans*, 113(C6): C06013, doi: 10.1029/2006jc004051.
- Gerringa L J A, Alderkamp A-C, Laan P, et al. 2012. Iron from melting glaciers fuels the phytoplankton blooms in Amundsen Sea (Southern Ocean): Iron biogeochemistry. *Deep Sea Res Part II*, 71-76: 16-31, doi: 10.1016/j.dsr2.2012.03.007.
- Li X, Gerber E P, Holland D M, et al. 2015. A Rossby wave bridge from the tropical Atlantic to West Antarctica. *J Clim*, 28(6): 2256-2273, doi: 10.1175/Jcli-D-14-00450.1.
- Loeb V, Hofmann E E, Klinck J M, et al. 2009. ENSO and variability of the Antarctic Peninsula pelagic marine ecosystem. *Antarct Sci*, 21(2): 135-148, doi: 10.1017/S0954102008001636.
- Loeb V, Hofmann E E, Klinck J M, et al. 2010. Hydrographic control of the marine ecosystem in the South Shetland-Elephant Island and Bransfield Strait region. *Deep Sea Res Part II*, 57(7/8): 519-542, doi: 10.1016/j.dsr2.2009.10.004.
- Marshall G J. 2003. Trends in the southern annular mode from observations and reanalyses. *J Clim*, 16(24): 4134-4143, doi: 10.1175/1520-0442(2003)016<4134:Titsam>2.0.Co;2.
- Prézelin B B, Hofmann E E, Moline M, et al. 2004. Physical forcing of phytoplankton community structure and primary production in continental shelf waters of the Western Antarctic Peninsula. *J Mar Res*, 62(3): 419-460, doi: 10.1357/0022240041446173.
- Saba G K, Fraser W R, Saba V S, et al. 2014. Winter and spring controls on the summer food web of the coastal West Antarctic Peninsula. *Nat Commun*, 5(1): 4318-4318, doi: 10.1038/ncomms5318.
- Schofield O, Brown M, Kohut J, et al. 2018. Changes in the upper ocean mixed layer and phytoplankton productivity along the West Antarctic Peninsula. *Philos Trans R Soc London Ser A*, 376(2122): 20170173, doi: 10.1098/rsta.2017.0173.
- Thomson R E, Emery W J. 2014. *Data analysis methods in physical oceanography*. San Diego: Elsevier Science & Technology.
- Venables H J, Clarke A, Meredith M P. 2013. Wintertime controls on summer stratification and productivity at the western Antarctic Peninsula. *Limnol Oceanogr*, 58(3): 1035-1047, doi: 10.4319/lo.2013.58.3.1035.
- Wasserman L. 2004. *All of statistics: a concise course in statistical inference*. New York: Springer.
- Zhang Z, Hofmann E E, Dinniman M S, et al. 2020. Linkage of the physical environments in the northern Antarctic Peninsula region to the Southern Annular Mode and the implications for the phytoplankton production. *Prog Oceanogr*, 188: 102416, doi: 10.1016/j.pocean.2020.102416.